Original Article

BIO Integration

Optimization of Ultra-Small Nanoparticles for Enhanced Drug Delivery

Shishi He[1,2,a], Yanni Fu[1,3,a], Zicong Tan[1,3], Qun Jiang[4,5], Kangling Huang[1,2], Phei Er Saw[1,6], Yan Nie[1,2,*] and Mingyan Guo[1,3,*]

Abstract

Nanoparticle delivery of drugs to the brain is hindered by the blood-brain barrier (BBB). In malignant glioma (MG), small disruptions in the BBB may allow nanoparticles smaller than 20 nm to penetrate the dysfunctional barrier. We previously developed ultra-small nanoparticles called hyper-cell permeable micelles (HCPMis) with a radius of ~12 nm and found that a PEGylated HCPMi system showed enhanced cell permeability and cellular uptake, and remarkable anti-tumor properties in MG treatment. However, no study had examined the delivery of temozolomide (TMZ), the first-line drug for MG, with the HCPMi platform. Herein, we use a simple PEGylation increment system (30 wt % PEG, 40 wt % PEG and 50 wt % PEG) to develop a robust optimized HCPMi nanoplatform for TMZ delivery. All optimized HCPMi systems showed greater stability than the non-PEGylated parent formulation. Compared with commercially available micelles (DSPE-PEG_{2000}), all optimized HCPMi systems showed greater cellular uptake *in vitro*. Although a higher percentage of PEGylation was associated with better cellular uptake and anti-cancer properties, the difference was statistically insignificant. Furthermore, *in vitro* cytotoxicity assays revealed that all optimized HCPMi-encapsulated TMZ formulations showed significantly stronger anti-cancer properties than the parent drug TMZ and TMZ encapsulated DSPE-PEG_{2000}, thus indicating the feasibility of using this nanoplatform for the delivery of TMZ to treat brain malignancies.

Keywords

Blood-brain barrier, hyper-cell permeable micelle, optimization, PEGylation, temozolomide, ultra-small nanoparticles.

[1]Guangdong Provincial Key Laboratory of Malignant Tumor Epigenetics and Gene Regulation, Guangdong-Hong Kong Joint Laboratory for RNA Medicine, Sun Yat-sen Memorial Hospital, Sun Yat-sen University, Guangzhou 510120, China

[2]Breast Tumor Center, Sun Yat-sen Memorial Hospital, Sun Yat-sen University, Guangzhou, 510120, China

[3]Department of Anesthesiology, Sun Yat-sen Memorial Hospital, Sun Yat-sen University, Guangzhou, 510120, China

[4]The Second Affiliated Hospital of Guangzhou University of Chinese Medicine, Guangzhou, 510120, China

[5]Department of Anesthesiology, University of Virginia, Charlottesville, VA 22908, U.S.A.

[6]Medical Research Center, Sun Yat-sen Memorial Hospital, Sun Yat-sen University, Guangzhou, 510120, China

[a]Shishi He and Yanni Fu contribute equally to this work.
*Correspondence to:
Mingyan Guo,
E-mail: guomyan@mail.sysu.edu.cn;
Yan Nie,
E-mail: nieyan7@mail.sysu.edu.cn

Received: April 21 2022
Revised: May 5 2022
Accepted: May 7 2022
Published Online: May 18 2022

Available at:
https://bio-integration.org/

Introduction

The blood-brain barrier (BBB) acts as both a physical and a biochemical barrier to drug delivery into the normal brain; thus, extensive efforts have been aimed at developing methods to modulate or bypass the BBB for the delivery of therapeutics [1]. Unfortunately, these efforts have not led to major changes in the landscape of brain disease therapy. Previous studies have revealed that the function and organization of the BBB is altered under pathological conditions, including stroke and brain cancer [2, 3], thus suggesting a potential for drug delivery into the brain. Some studies have found that malignant glioma (MG) induces small disruptions in the integrity of the BBB; however, many parent drugs remain unavailable or are inefficient in crossing the BBB, thus making drug therapy for MG very difficult [4–6]. Temozolomide (TMZ), the first-line drug for the treatment of MG, is hindered by the BBB, which significantly weakens its anti-cancer properties and promotes systemic toxicity. Therefore, facilitating the passage of TMZ across the dysfunctional BBB and decreasing systemic toxic effects are goals for treating MG.

Recently, nanoparticles have been demonstrated to have excellent ability to penetrate the dysfunctional BBB and thus might serve as an ideal carrier for delivering drugs into the central nervous system. The BBB is slightly compromised in MG, thereby allowing the passage of nanocarriers smaller than 20 nm [7–9].

Lipid-based drug delivery vehicles, including liposomes and micelles, have been intensively studied and widely used for multiple biomedical applications, such as cancer therapy [10–12]. As drug carriers, nanoparticles have unique benefits, including protecting drugs against degradation in the circulation and decreasing systemic toxic effects. Moreover, owing to their small diameters, nanoparticles can penetrate through the fissures in intratumor vessels into tumors and remain there

BIOI 2023, Vol 4, No. 2, 62–69
https://bio-integration.org doi: 10.15212/bioi-2022-0015

because of the obstruction of tumor lymphatic drainage—a phenomenon known as the enhanced permeability and retention effect [13, 14]. Previous studies have indicated that polyethylene glycol (PEG) modification decreases intermolecular interactions and the immunogenicity of nanoparticles, thereby increasing the stability of nanoparticles *in vivo* and decreasing phagocytosis [15]. PEGylation has been widely used to optimize drug delivery carriers and improve the retention and concentration of drugs in circulation. Li and colleagues have synthesized a new shielding material by conjugating PEG to a hyaluronic acid core for gene delivery applications [16]. In our previous study, we modified the formulation, adding 10 wt % of DMPE-PEG_{2000} to the system for formulating disc-shaped bicelles (BCs), thus yielding uniformly distributed ultra-small (~12 nm) spherical micelles, which we termed hyper-cell-permeable micelles (HCPMis). HCPMis may serve as an ideal vehicle for delivering antitumor drugs because of their small diameter, high stability and absence of major cytotoxicity, as well as their ability to penetrate and accumulate in tumors through rapid cellular uptake [17]. Therefore, HCPMis with a size of only approximately 12 nm may be effective carriers for delivering TMZ across the BBB and decreasing systemic adverse effects, thus providing a new prospective MG treatment.

Each nanoparticle system has an optimal percentage of PEG [13]. For example, 10 wt % PEG for poly (lactic acid) nanoparticles and poly (lactide-co-glycolide) nanoparticles improves particle dispersibility and the stealth effect [18, 19]. Furthermore, PEG formulations of nanoparticles are associated with circulation duration *in vivo*. One study comparing the stability of two formulations of nanoparticles with 10 wt % PEG and 30 wt % PEG in mice has found that nanoparticles containing 30 wt % PEG are retained longer in the systemic circulation [20]. However, excess PEG may affect nanoparticles stability and decrease cellular uptake [13, 21]. For example, our previous study has indicated that in BxPC3 and SCC-7 cells, 10 wt % PEGylated HCPMi shows greater cellular uptake than 20 wt % PEGylated HCPMi [17]. At present, no study has examined in the delivery TMZ for MG treatment with the HCPMi platform. Herein, to obtain nanoparticles with both high stability and rapid cellular uptake rates for TMZ delivery, we used a simple PEGylation increment system (30 wt % PEG, 40 wt % PEG and 50 wt % PEG) to develop a robust and optimized HCPMi nanoplatform for TMZ delivery.

Materials and methods

Materials

The 1,2-dihexanoyl-sn-glycero-3-phosphocholine (DHPC), 1,2-dimyristoyl-sn-glycero-3-phosphocholine (DMPC), 1,2-dimyristoyl-sn-glycero-3-phosphoethanolamine-N-(lissamine rhodamine B sulfonyl) (ammonium salt) (Rh-DMPE), 1,2-dimyristoyl-sn-glycero-3-phosphoethanolamine-N-[methoxy(polyethylene glycol)-2000] (ammonium salt) (DMPE-PEG_{2000}), 1,2-distearoyl-sn-glycero-3-phosphoethanolamine-N-[methoxy(polyethylene glycol)-2000] (ammonium salt) (DSPE-PEG_{2000}) and a mini-extrusion set were purchased from Avanti Polar Lipids (Alabama, USA). Uranyl acetate and temozolomide were purchased from Sigma-Aldrich (MA, USA). DAPI staining solution was purchased from Vectashield (MI, USA). All chemicals and reagents were purchased from Sigma Aldrich (MA, USA) unless stated otherwise.

Preparation of nanoparticles

As reported previously, we confirmed that two phospholipids used for BC formation—a long-chain phospholipid with 14-carbon lipid tails (DMPC) and a short-chain phospholipid with 6-carbon lipid tails (DHPC)—self-assembled to form typical bicellar disc shapes (**Figure 1A**). BCs were prepared by mixture of DMPC and DHPC dissolved in chloroform at a ratio of 3:1 to yield a 2 mg/mL solution; drying to obtain a lyophilized lipid mixture; and dissolving in 1 mL PBS solution. PEG was added to each formulation at the indicated molar percentage of the HCPMi. For example, for a 30% PEGylated HCPMi, a 10 mg/mL HCPMi (8 μM) contained 3 mg of DMPE-PEG_{2000} (0.001 μM). Similarly, 40% and 50% PEGylated HCPMi were prepared by addition of 4 mg and 5 mg DMPE-PEG_{2000}, respectively. The DSPE-PEG_{2000} was used as received. Similarly to HCPMi, DSPE-PEG_{2000} was first dissolved in chloroform at a 100 mg/mL concentration. Then 10 mg of DSPE-PEG_{2000} from the stock vial was transferred to a glass vial. After freeze-drying (or open air-drying), a lipid film formed at the bottom of the glass vial. After addition of 1 mL of PBS, the DSPE-PEG_{2000} spontaneously formed with constant stirring. Rhodamine-labeled nanoparticles were prepared by addition of 0.5 wt % of rhodamine-DMPE. The fluorescence intensity of each group was assessed with a spectrophotometer and normalized (Thermo).

Transmission electron microscopy (TEM) analysis

Nanoparticles (10 μL) were applied to TEM-grade carbon-only mesh copper grids for 5 min, and excess samples was blotted with filter paper. After being washed five times with distilled water, each grid was negatively stained with 10 mL of 1% uranyl acetate for 2 min. The samples were washed three times with distilled water and dried. Then the samples were observed under a transmission electron microscope (Philips) at 200 kV.

In vitro drug release tests

To determine the drug release profile of each PEGylated HCPMi and DSPE-PEG_{2000}, we used cumulative addition of released rhodamine fluorescence as an indicator of release. First, 10 mg/mL of each formulation were added into a Float-a-lyzer device (100 kDa). At specific time points (5, 15, 60 min, 2, 4, 12, 24, 48 and 96 h), the fluorescence intensity

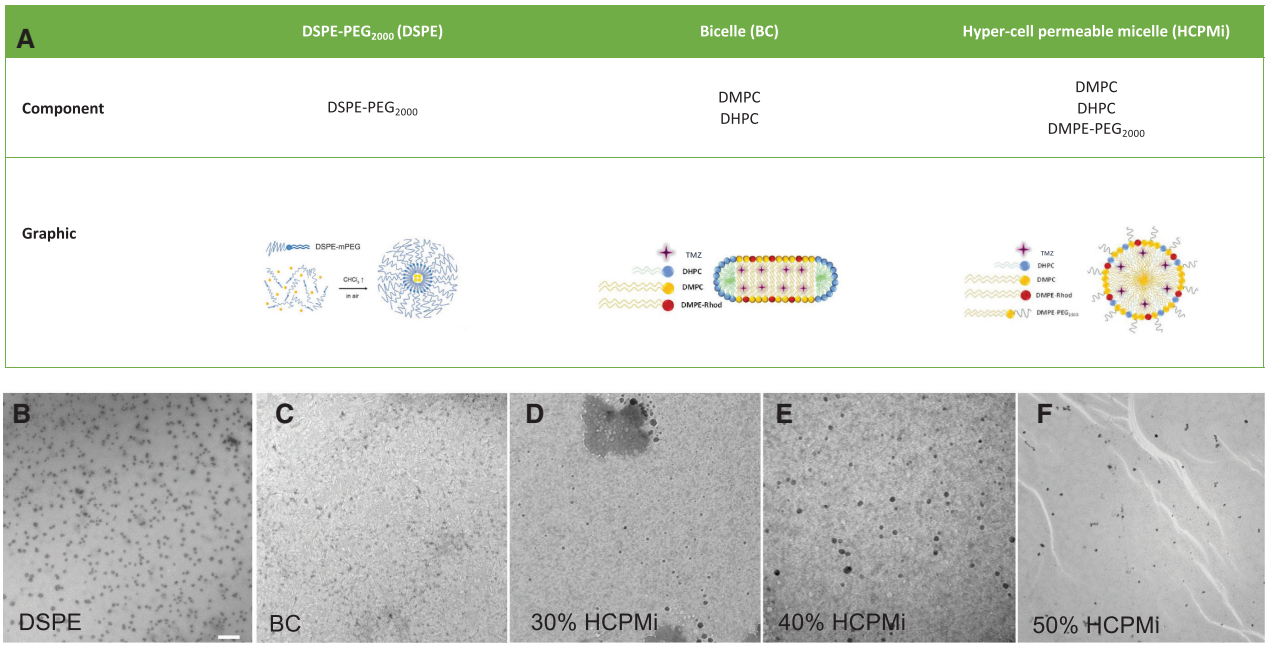

Figure 1 Graphic representation and morphology of the commercial DSPE, BCs and HCPMis. (A) The graphic shows the transformation of BC structure into spherical micelles with the addition of DMPE-PEG_{2000}. (B–F) TEM analysis of the morphology of DSPE (100 wt % PEG), BC (0 wt % PEG) and 30–50 wt % PEGylated HCPMi. Scale bar, 2 µm.

from the outer buffer was determined and used to obtain the profile in **Figure 3**.

In vitro stability tests

A 900 µL volume of nanoparticle solution was placed in a transparent cuvette, and 100 µL of fetal bovine serum (Gibco) was added to make a 10% solution. The solution was sealed and placed on a shaker at 37°C. The sizes of nanoparticles were detected through dynamic light scattering (DLS; Malvern Panalytical) after 0 h, 1 h, 4 h, 24 h and 96 h incubation.

Encapsulation efficiency

TMZ was dissolved in methanol to generate a 1 mg/mL solution for encapsulation. TMZ solution was added to the solution for preparing nanoparticles, dried to remove solvents and dissolved in PBS solution. Then the solution was filtered through a 0.2 µm polycarbonate membrane syringe filter to remove unencapsulated TMZ from the solution. The concentration of TMZ in the solution was determined, and the loading TMZ encapsulation efficiency was calculated as follows: encapsulation efficiency = (amount of TMZ after filtration)/(amount of TMZ before encapsulation).

In vitro cell uptake assays

The glioma cell lines U87MG and U251MG were cultured in DMEM containing 10% fetal bovine serum. Cells were treated with 100 µg/mL rhodamine-labeled nanoparticles and incubated at 37°C. After 1 h of incubation, the cells were fixed with 4% paraformaldehyde, and the nuclei were labeled with DAPI. Cells were imaged under 400× magnification with a confocal laser scanning microscope (Zeiss LSM 710).

Cell cytotoxicity assays

U87MG and U251MG cells were seeded in 96-well plates at 3000 cells per well. After 12 h of culture, cells were treated with TMZ or TMZ-encapsulated nanoparticles for 12–48 h. The cells were then washed twice with PBS and cultured for 24 h. The cell viability of each group was detected with CCK8 (Apex BIO) assays.

Statistical analysis

The data were statistically analyzed in SPSS 25.0 software (SPSS Inc., Chicago, IL). The normal distribution of data from parametric results was confirmed through Kruskal Wallis analysis of variance of ranks followed by Tukey's or Dunn's test when the data were not normally distributed, or by Student's *t*-test as appropriate. After confirmation, the results were analyzed with *t*-test or one-way analysis of variance followed by Tukey's test. Data are displayed as mean ± standard deviation, and $P < 0.05$ was the threshold for statistical significance.

Results

Formation and morphology of BCs and HCPMis

We used DMPC and DHPC for BC formation, as reported previously. DMPC is a long-chain phospholipid with

14-carbon lipid tails, whereas DHPC is a short-chain phospholipid with 6-carbon lipid tails. The two phospholipids self-assemble into typical bicellar disc shapes. In our previous study, 10 wt % DMPE-PEG_{2000} was added to the BC-forming formulation, and compact and spherical HCPMis were synthesized (**Figure 1A**). Herein, we changed the percentage of PEGylation for further optimizing HCPMis, applying 30 wt %, 40 wt % or 50 wt % of DMPE-PEG_{2000} in the formulations, and successfully produced typical spherical micellar nanoparticles. TEM analysis was performed to assess the morphology of DSPE, BCs and PEGylated HCPMis, and all PEGylated HCPMis were found to be spherical (**Figure 1B–E**).

Encapsulation efficiency of DSPE, BCs and HCPMis

TMZ loading efficiency was determined through filtration and UV spectrophotometry. The results indicated 98.7% loading in DSPE, 89.7% loading in BCs, 97.7% loading in 30% PEGylated HCPMis, 90.6% loading in 40% PEGylated HCPMis and 88.8% loading in 50% PEGylated HCPMis. As expected, each nanoparticle had an optimal percentage of PEG. The encapsulation efficiency of PEGylated HCPMis decreased with increasing PEG, although the difference was not significant. Thus, 30% PEGylated HCPMi showed better (or at least not worse) efficiency than the higher PEGylated HCPMis, as well as the BCs. The commercial DSPE showed the highest encapsulation efficiency among all five particles, although the difference was not significant (**Table 1**).

Stability and size of BCs and PEGylated HCPMis

The feasibility of HCPMi as a drug-delivery carrier was further investigated. Among the various features, nanoparticles stability in solution is crucial for drug delivery. To determine whether the PEG component affected HCPMi stability, we added 10% fetal bovine serum to the solutions of BCs and optimized HCPMis, then observed the changes and particle sizes in the solutions via DLS. The BC solution became turbid after the addition of serum, and precipitates were visible 96 h later, whereas the other three PEGylated HCPMi solutions remained stable and clear (**Figure 2A**). DLS analysis indicated that the radius of BC was 60 nm, and the radii of the three PEGylated HCPMis (30 wt % PEG, 40 wt % PEG and 50 wt % PEG) were 12 nm, 11 nm and 14 nm, respectively. The PEGylated HCPMi solutions maintained a particle size

Table 1 Encapsulation Efficiency of DSPE, BCs and PEGylated HCPMis

	Input (A.U.)	DSPE (A.U.)	BC (A.U.)	30% HCPMi[a] (A.U.)	40% HCPMi[a] (A.U.)	50% HCPMi[a] (A.U.)
Repeat 1	2392	2830	2096	2761	2757	2975
Repeat 2	3002	2971	2643	2792	2659	2595
Repeat 3	2674	2654	2579	2791	2827	2737
Repeat 4	2929	2846	2721	2744	2572	2314
Repeat 5	3405	2917	2885	2985	2231	2168
Average	2880.4	2843.6	2584.8	2814.6	2609.2	2557.8
Encapsulation efficiency (%)	100	98.7	89.7	97.7	90.6	88.8

[a] 30 wt %, 40 wt % and 50 wt % PEGylated HCPMis are displayed as 30%, 40% and 50% HCPMi, respectively.

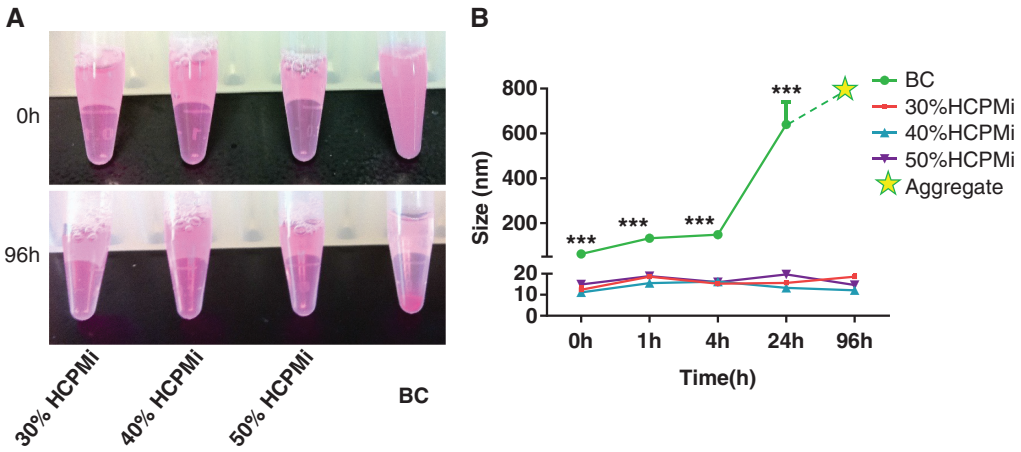

Figure 2 Stability analysis of BCs and PEGylated HCPMis. (A) The stability of HCPMis compared with BCs at ambient temperature. The image was taken after 96 hours of incubation of each formulation in FBS solution. BCs showed aggregates at the bottom of the microcentrifuge tube, thus suggesting instability. The HCPMi solution remained clear in the colloidal state, thereby indicating high stability in FBS solution. (B) DLS detection of the radii of BCs and HCPMis in solutions containing 10% serum. The PEGylated HCPMis were stable in size, whereas the BC particles gradually increased in size and finally aggregated, thus indicating that BCs are too unstable to serve as a drug carrier. The 30 wt %, 40 wt % and 50 wt % PEGylated HCPMis are displayed as 30%, 40% and 50% HCPMi, respectively. ***$P < 0.001$ compared with the control. Bars correspond to mean ± S.D.

below 20 nm, thus suggesting that these nanoparticles stably maintained a monomeric state in the colloidal solution (**Figure 2B**). These results indicated that optimization of the addition of PEG to the BC formulation decreased the size and increased the stability of nanoparticles in colloidal solutions, with no adsorption or aggregation.

TMZ release profile in DSPE and PEGylated HCPMis

BCs were unstable in solution and thus were an unsuitable intravenous drug carrier. To evaluate the stability of nanoparticles loaded with TMZ, we tested the release profiles of DSPE and the three PEGylated HCPMis. We determined the concentrations of residual TMZ in nanoparticles at different time points (5, 15, 60 min, 2, 4, 12, 24, 48 and 96 h) through HPLC analysis and calculated the TMZ release amounts at different times. The release profiles of the three PEGylated HCPMis were similar to those of commercial DSPE, thus indicating that the PEGylated HCPMis could be stably loaded with TMZ for at least 48 h (**Figure 3**).

In vitro cellular uptake and cytotoxicity of DSPE and PEGylated HCPMis in the U87MG and U251MG cell lines

We continued to explore whether different PEGylation percentages affected cellular HCPMi uptake. Our previous study has indicated that in SSC-7oral squamous cell carcinoma and BxPC3pancreatic cancer cells, an increase in PEGylation increases the cellular HCPMi uptake within the range of 4 wt % to 10 wt % [17]. Therefore, we wondered whether this phenomenon could be observed in MG cells, and whether higher levels of PEGylation might influence cellular HCPMi uptake. For this purpose, we added rhodamine-labeled HCPMis with 30%, 40% or 50% PEGylation to the *in vitro* cultured human glioma cell lines U87MG and U251MG. DSPE was used as a control. After 1 h of incubation, the cellular uptake of nanoparticles was observed through confocal microscopy. The cells in the DSPE group showed almost no fluorescence signal, whereas the intracellular fluorescence intensity significantly accumulated in all three PEGylated HCPMi, thus indicating that the cellular uptake properties of optimized HCPMis were much better than those of DSPE; therefore these systems served as competent drug carriers (**Figure 4A,B**). We further analyzed the ability of PEGylated HCPMi to deliver TMZ for the treatment of MG. We compared the cytotoxicity of the optimized HCPMi with DSPE on U87MG and U251MG cells *in vitro*. The cytotoxicity of all three PEGylated HCPMis was significantly stronger than that of DSPE and increased with the TMZ concentration (from 0.3125 μM to 1.25 μM). Interestingly, when the concentration of TMZ reached 1.25 μM, the cytotoxicity of the HCPMi plateaued, thus indicating that as a drug carrier, the highest TMZ content that HCPMi can deliver is determined, which is not vary with the different PEG content (**Figure 4C,D**).

In vitro cytotoxicity of TMZ encapsulated in BCs, DSPE and 30% PEGylated HCPMis, as compared with the parent drug

Because 30% PEGylated HCPMi showed almost the same stability, cellular uptake and cytotoxicity as the 40% and 50% PEGylated HCPMis, considering the balance of effects and cost, we chose 30% PEGylated HCPMi as the optimized carrier for further validation. We analyzed the ability of PEGylated HCPMi to deliver TMZ for the treatment of MG. We compared the cytotoxicity of four forms of TMZ—parent drug, BC, DSPE and 30% PEGylated HCPMi-encapsulated TMZ—in U87MG cells *in vitro* by assaying cell viability. The 30% PEGylated HCPMi-encapsulated TMZ showed the best cytotoxic effects against MG when the TMZ concentration reached 1.25 μM (**Figure 5**).

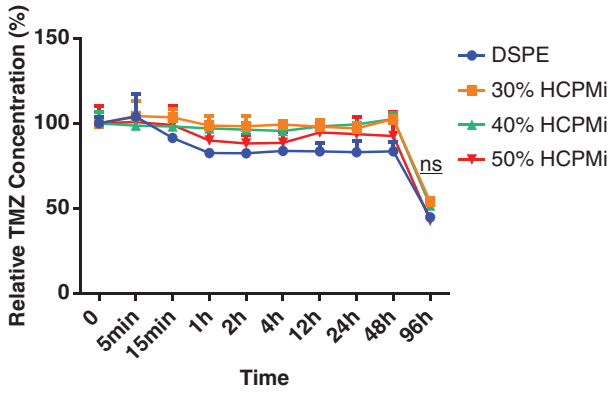

Figure 3 TMZ release profile in DSPE and PEGylated HCPMis. Concentrations of TMZ in DSPE and three PEGylated HCPMis at the indicated time points (5, 15, 60 min, 2, 4, 12, 24, 48 and 96 h). The 30 wt %, 40 wt % and 50 wt % PEGylated HCPMis are displayed as 30%, 40% and 50% HCPMi, respectively. N.s. indicates nonsignificant compared with the control. Bars correspond to mean ± S.D.

Discussion

In this study, we aimed to develop a robust and optimized HCPMi nanoplatform, based on our previous formation of HCPMi, for TMZ delivery [17]. We used a simple PEGylation increment system (30 wt % PEG, 40 wt % PEG and 50 wt % PEG) and non-PEGylated BCs and commercially available DSPE as controls. All optimized HCPMi had smaller radii and were significantly more stable than BCs. Moreover, all PEGylated HCPMis showed better cellular uptake and higher cytotoxicity than DSPE, thus indicating that PEGylated HCPMis are ideal nanocarriers for delivering TMZ for MG treatment. PEG forms a flexible layer on the nanoparticle surface and is widely used to increase the stability of nanoparticles and prevent their engulfment by immune cells [13]. Every nanoparticle system has an optimal formulation: although higher PEG

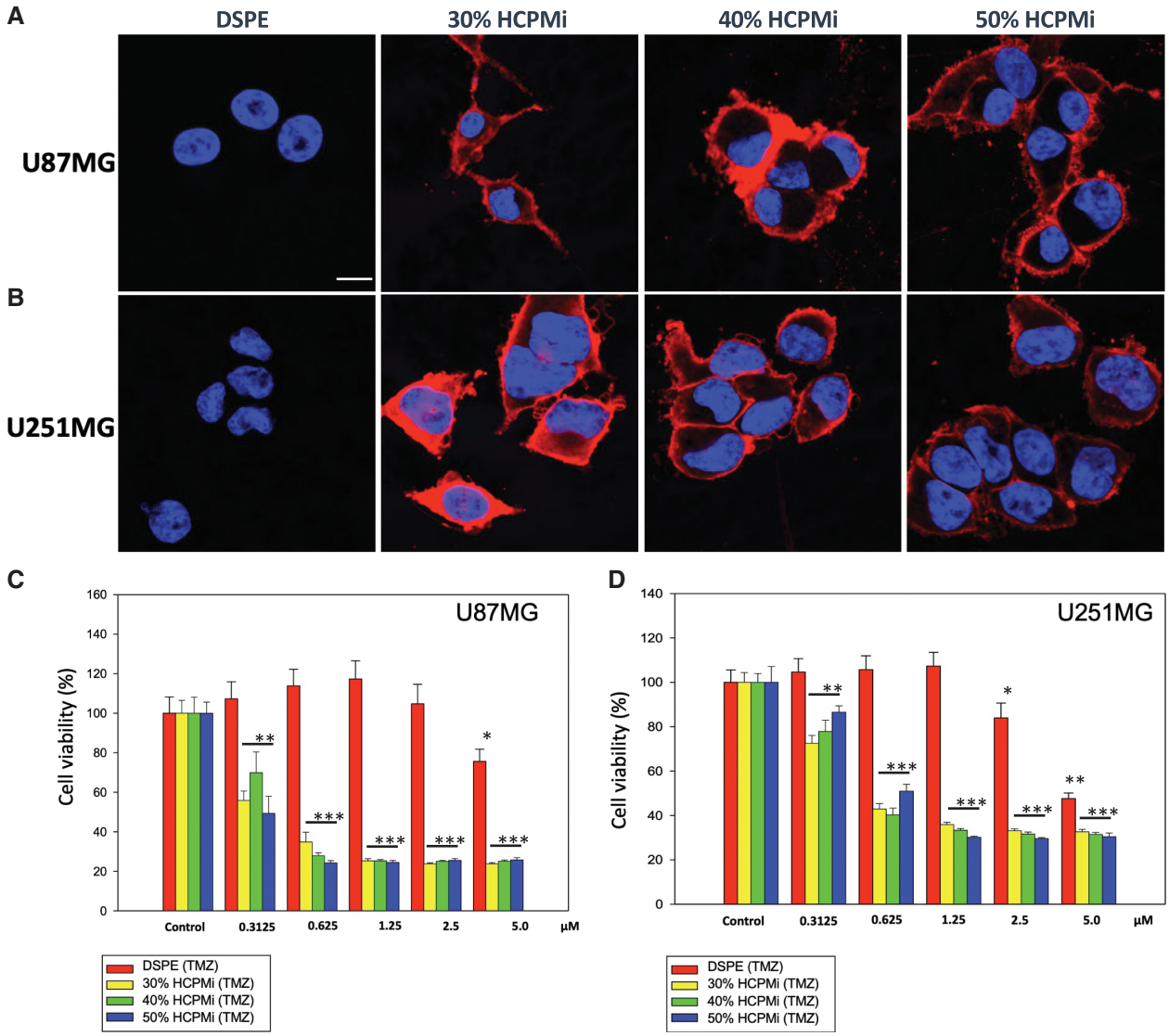

Figure 4 *In vitro* cellular uptake and cytotoxicity of DSPE and PEGylated HCPMis in the U87MG and U251MG cell lines. (A) Rhodamine intracellular fluorescence intensity in U87MG cells; scale bar, 20 μm. (B) Rhodamine intracellular fluorescence intensity in U251MG cells; scale bar, 20 μm. (C) Cytotoxicity of DSPE and optimized HCPMi in U87MG cells. (D) Cytotoxicity of DSPE and optimized HCPMi in U251MG cells. The 30 wt %, 40 wt % and 50 wt % PEGylated HCPMis are displayed as 30%, 40% and 50% HCPMi, respectively. $^{*}P < 0.05$, $^{**}P < 0.01$ and $^{***}P < 0.001$ compared with the control. Bars correspond to mean ± S.D.

content may improve the stability of nanoparticles, it also may decrease the cellular uptake rate [21]. Our previous study has indicated similar cellular HCPMi uptake in the range of 4–10 wt % PEG in both BxPC3 and SCC-7 cell lines, but a significantly lower cellular uptake with a PEG content exceeding 10 wt % [17]. These findings are mainly because the exclusion among PEG chains increases with the PEG content and may alter the structure of the nanoparticles and thus affect cellular uptake rates [21]. Herein, we observed similar stability and MG cellular uptake with the 30–50 wt % PEGylation increment system, whereas 30% PEGylated HCPMi showed the highest encapsulation, although the difference was insignificant. To balance cost and effects, we chose the 30% PEGylated HCPMi for further research. We then compared the cytotoxicity of TMZ encapsulated in 30% PEGylated HCPMis, BCs or DPSE with the parent TMZ. Among these treatments, TMZ encapsulated in 30% PEGylated HCPMi had the highest cytotoxicity toward U87MG cells at a very low concentration of 1.25 μM.

MG is a malignant tumor that affects the central nervous system and results in a high incidence of mortality and disability due to neurological injury. In surgical treatment, MG is difficult to remove cleanly, and local recurrence usually occurs. Moreover, chemotherapeutics, such as the first-line drug, TMZ, are hindered by the BBB, thus resulting in insufficient local drug concentration and poor patient prognosis [4–6]. The development of nanoparticle delivery systems in recent years has provided new prospects for drug treatment of MG. The use of small nanoparticle encapsulated drugs can improve the stability of drugs *in vivo*, increase the blood concentration, and promote drug penetration of the BBB [7–9]. In addition, the use of PEGylated nanoparticles can make the nanoparticles more stable. We prepared HCPMi nanoparticles PEGylated with a high percentage of PEG to prolong their retention in the blood circulation, and enhance

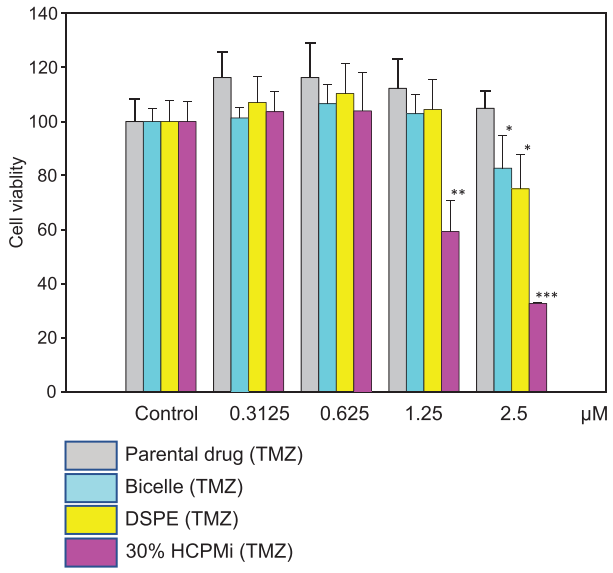

Figure 5 *In vitro* cytotoxicity of TMZ encapsulated in BCs, DSPE and 30% PEGylated HCPMis, compared with the parent drug, in the U87MG cell line. Cytotoxicity of four forms of TMZ (parent drug, BC, DSPE and 30% PEGylated HCPMi-encapsulated TMZ) on U87MG cells *in vitro*, on the basis of cell viability assays. The 30% PEGylated HCPMi-encapsulated TMZ had the best cytotoxic effect against MG when the TMZ concentration reached 1.25 μM. The 30 wt %, 40 wt % and 50 wt % PEGylated HCPMis are displayed as 30%, 40% and 50% HCPMi, respectively. $^{*}P < 0.01$, $^{**}P < 0.01$ and $^{***}P < 0.001$ compared with the control. Bars correspond to mean ± S.D.

their penetration of the BBB. When nanocarriers are used to encapsulate TMZ, they can increase the local drug concentration in tumors and promote cytotoxicity. However, every HCPMi has an optimized amount of PEGylation. In this study, HCPMi nanoparticles less than 15 nm were formed with application of 30%, 40% or 50% PEGylated phospholipids, none of which significantly affected nanoparticle size and stability. Because 30%, 40% and 50% PEGylation of HCPMis showed no significant differences according to size, stability, cellular uptake and cytotoxicity, to balance the effects and costs, we chose the optimal HCPMis with 30% PEGylation for further research.

Our previous results have shown that PEGylated HCPMi has a small radius, stable properties, and a long half-life in the blood stream [17]. Therefore, it might serve as a carrier for drug delivery in the treatment of neurological diseases such as epilepsy, stroke and Parkinson's disease, as well as MG. Moreover, PEGylated HCPMi could also be applied for the delivery of nucleic acid drugs. Its stability *in vivo* could protect siRNAs, ASOs, lncRNAs and other nucleic acids from degradation, and prolong the half-life of nucleic acid drugs *in vivo*. The ultra-small size confers PEGylation optimized HCPMis with high permeability and long retention times in tumors, thus potentially improving the efficiency of delivery of nucleic acid drugs to tumors. The PEGylation percentage of HCPMi could be optimized in additional cells in future studies. The combination of optimized HCPMis and nucleic acid drugs may provide new targeted therapeutic options for various refractory diseases and tumors.

However, this study has several limitations. First, the gradient of PEGylation was relatively small, although 30 wt % PEG added to HCPMi was sufficient to achieve excellent drug carrier properties. We plan to test more PEGylation gradients between 20 wt % and 40 wt % to analyze the radius, stability and uptake ability of the optimized HCPMis by MG cells to identify the most optimal PEGylation conditions. Second, we did not perform *in vivo* analysis of the effects of HCPMis on MG after TMZ encapsulation. Therefore, we will further establish an *in vivo* model of MG to evaluate the efficacy of optimized HCPMi-encapsulated TMZ for the treatment of MG, to provide additional evidence of PEGylated HCPMi as a potentially feasible carrier for brain malignancy.

Conclusions

Our results indicated that 30% PEGylation showed the best TMZ encapsulation and cellular uptake, although *in vitro* cytotoxicity assays revealed that all optimized HCPMi-encapsulated TMZ showed greater anti-cancer properties than the parent drug TMZ and TMZ encapsulated DSPE. This ultra-small nanoplatform may be used for the delivery of other drugs across the BBB for the treatment of brain malignancies.

References

[1] Larsen JM, Martin DR, Byrne ME. Recent advances in delivery through the blood-brain barrier. Curr Top Med Chem 2014;14:1148-60. [PMID: 24678707 DOI: 10.2174/1568026614666140329230311]

[2] Zlokovic BV. The blood-brain barrier in health and chronic neurodegenerative disorders. Neuron 2008;57:178-201. [PMID: 18215617 DOI: 10.1016/j.neuron.2008.01.003]

[3] Daneman R. The blood-brain barrier in health and disease. Ann Neurol 2012;72:648-72. [PMID: 23280789 DOI: 10.1002/ana.23648]

[4] Sarkaria JN, Hu LS, Parney IF, Pafundi DH, Brinkmann DH, et al. Is the blood-brain barrier really disrupted in all glioblastomas? A critical assessment of existing clinical data. Neuro Oncol 2018;20:184-91. [PMID: 29016900 DOI: 10.1093/neuonc/nox175]

[5] Arvanitis CD, Ferraro GB, Jain RK. The blood-brain barrier and blood-tumour barrier in brain tumours and metastases. Nat Rev Cancer 2020;20:26-41. [PMID: 31601988 DOI: 10.1038/s41568-019-0205-x]

[6] Achar A, Myers R, Ghosh C. Drug delivery challenges in brain disorders across the blood-brain barrier: novel methods and future considerations for improved therapy. Biomedicines 2021;9. [PMID: 34944650 DOI: 10.3390/biomedicines9121834]

[7] Li J, Cai P, Shalviri A, Henderson JT, He C, et al. A multifunctional polymeric nanotheranostic system delivers doxorubicin and imaging agents across the blood-brain barrier targeting brain metastases of breast cancer. ACS Nano 2014;8:9925-40. [PMID: 25307677 DOI: 10.1021/nn501069c]

[8] Li W, Qiu J, Li XL, Aday S, Zhang J, et al. BBB pathophysiology-independent delivery of siRNA in traumatic brain injury. Sci Adv 2021;7. [PMID: 33523853 DOI: 10.1126/sciadv.abd6889]

[9] Ugur Yilmaz C, Emik S, Orhan N, Temizyurek A, Atis M, et al. Targeted delivery of lacosamide-conjugated gold nanoparticles into the brain in temporal lobe epilepsy in rats. Life Sci 2020;257:118081. [PMID: 32663576 DOI: 10.1016/j.lfs.2020.118081]

[10] Bhattacharyya S, Ahmmed SM, Saha BP, Mukherjee PK. Soya phospholipid complex of mangiferin enhances its hepatoprotectivity by improving its bioavailability and pharmacokinetics. J Sci Food Agric 2014;94:1380-8. [PMID: 24114670 DOI: 10.1002/jsfa.6422]

[11] Chay SY, Tan WK, Saari N. Preparation and characterisation of nanoliposomes containing winged bean seeds bioactive peptides. J Microencapsul 2015;32:488-95. [PMID: 26079597 DOI: 10.3109/02652048.2015.1057250]

[12] Jantscheff P, Esser N, Graeser R, Ziroli V, Kluth J, et al. Liposomal gemcitabine (GemLip)-efficient drug against hormone-refractory Du145 and PC-3 prostate cancer xenografts. Prostate 2009;69:1151-63. [PMID: 19399788 DOI: 10.1002/pros.20964]

[13] Amoozgar Z, Yeo Y. Recent advances in stealth coating of nanoparticle drug delivery systems. Wiley Interdiscip Rev Nanomed Nanobiotechnol 2012;4:219-33. [PMID: 22231928 DOI: 10.1002/wnan.1157]

[14] Maeda H, Wu J, Sawa T, Matsumura Y, Hori K. Tumor vascular permeability and the EPR effect in macromolecular therapeutics: a review. J Control Release 2000;65:271-84. [PMID: 10699287 DOI: 10.1016/s0168-3659(99)00248-5]

[15] Suk JS, Xu Q, Kim N, Hanes J, Ensign LM. PEGylation as a strategy for improving nanoparticle-based drug and gene delivery. Adv Drug Deliv Rev 2016;99:28-51. [PMID: 26456916 DOI: 10.1016/j.addr.2015.09.012]

[16] Liu J, Bao X, Kolesnik I, Jia B, Yu Z, et al. Enhancing the in vivo stability of polyanion gene carriers by using PEGylated hyaluronic acid as a shielding system. BIO Integration 2022. [DOI: 10.15212/bioi-2021-0033]

[17] Saw PE, Yu M, Choi M, Lee E, Jon S, et al. Hyper-cell-permeable micelles as a drug delivery carrier for effective cancer therapy. Biomaterials 2017;123:118-26. [PMID: 28167390 DOI: 10.1016/j.biomaterials.2017.01.040]

[18] Beletsi A, Panagi Z, Avgoustakis K. Biodistribution properties of nanoparticles based on mixtures of PLGA with PLGA-PEG diblock copolymers. Int J Pharm 2005;298:233-41. [PMID: 15936907 DOI: 10.1016/j.ijpharm.2005.03.024]

[19] Sheng Y, Yuan Y, Liu C, Tao X, Shan X, et al. In vitro macrophage uptake and in vivo biodistribution of PLA-PEG nanoparticles loaded with hemoglobin as blood substitutes: effect of PEG content. J Mater Sci Mater Med 2009;20:1881-91. [PMID: 19365612 DOI: 10.1007/s10856-009-3746-9]

[20] Mosqueira VC, Legrand P, Morgat JL, Vert M, Mysiakine E, et al. Biodistribution of long-circulating PEG-grafted nanocapsules in mice: effects of PEG chain length and density. Pharm Res 2001;18:1411-9.

[21] Tirosh O, Barenholz Y, Katzhendler J, Priev A. Hydration of polyethylene glycol-grafted liposomes. Biophys J 1998;74:1371-9. [PMID: 9512033 DOI: 10.1016/S0006-3495(98)77849-X]